International Journal of Engineering Research & Technology (IJERT)
ISSN: 2278-0181
Vol. 14, Issue 06, ACSCON - 2026

Investigations on Stresses and Displacements of Annular Rotating Disc using FEA

Tejas V[1], Nikhil Das S[1],
Dr. H S Siddesha[2]
[1]Student, Mechanical Engineering Department,ACSCE,Bangalore-74
[2]Professor,Mechanical Engineering Department,ACSCE,Bangalore-74
Email: skphss@gmail.com

Abstract - Engineering components that can be modeled as a rotating disc include the rotor of a turbine engine, saw blades, grinding wheels, and computer magnetic recording disks etc. The rotating disc is subjected to centrifugal force which tends to pull the disc in radial direction, introduces large stresses and displacements on the disc. Further the disc is mounted on a shaft by interference fit. The stresses and displacements of the rotating disc are estimated for potential boundary conditions by building a finite element model using ANSYS. The disc is meshed using SOLID45 elements by taking the rotating disc to be 3D cyclic symmetric model. The contact simulation is done for shaft and disc using surface to surface contacts in ANSYS. The linear isotropic material model is used.

The model creation for the given dimension with the required material properties is done by APDL (Ansys Parametric Design Language) macro. The user inputs the dimensions of the disc in the macro, which takes care of the model preparation, mesh generation, applying boundary conditions, solution and post processing for the load case. This gives flexibility to change the parameters and material properties according to user specification and saves time for finite element model preparation.

Key words: Cyclic symmetry, Plane stress, Plane strain, Interference fit, surface to surface contact.

1. INTRODUCTION

The Finite element method has become a powerful tool for numerical solution of a wide range of engineering problems. Applications range from deformation and stress analysis of automotive, aircraft, building and bridge structures to field analysis of heat flux, magnetic flux, and fluid flow problems. With advances in computer technology and CAD/CAE systems, complex problems can be modeled with relative ease. Several alternative configurations can be tried out on a computer before the first prototype is built. In finite element analysis, a complex region defining continuum is discretized into simple geometric shapes called finite elements. The material properties and the governing relationships are considered over these elements and expressed in terms of unknown values at element corners. An assembly process, duly considering the loading and constraints, results in a set of equations. Solution to these equations gives us the approximate behavior of the continuumThe problem of rotating disc was investigated for various conditions, as fallows:

Eraslan and Orcan [1] investigated rotating variable thickness elastoplastic annular disks with inner boundaries subject to pressure or mounted on rigid inclusion parametrically and developed computer model based on von mises criterion, deformation theory and non linear isotropic hardening. Eraslan [2] investigated A Class of Nonisothermal Variable Thickness Rotating Disk Problems Solved by Hypergeometric Functions. Exact solutions for nonisothermal variable thickness rotating disks represented by different thickness profiles are obtained under plane stress assumption. The solutions are based on Tresca's yield criterion, its associated flow rule and linear strain hardening material behavior. D.W.Cameron,P.R.Geise, J.S.Abbott [3] ,

(This work is licensed under a Creative Commons Attribution 4.0 International License.)

International Journal of Engineering Research & Technology (IJERT)
ISSN: 2278-0181
Vol. 14, Issue 06, ACSCON - 2026

presented method of setting centrifugal impeller over speed limits. The primary means of this determination is based on invoking yield criterion to control stresses.

2. FEA modeling using ANSYS

2.1 Modeling of rotating disc

The cyclic symmetric model of the disc is modeled using ANSYS APDL macro the mode is meshed using SOLID45 Element. A cyclic symmetry analysis requires that you model a single sector, called the basic sector. A proper basic structure represents one part of the a pattern that, if repeated N times in cylindrical coordinate system, yields the complete model. Analysis is carried out with csys1 with X,Y&Z axis set as Radial, Hoop & Axial directions respectively.

2.2 Meshing conditions

The model is meshed with SOLID45 elements with no wedges or tetrahedron element, with minimum 3 elements along thickness to capture bending behavior. The interference between the shaft and the disc is meshed to have matching nodes along the bore. This is required for generating contact and target elements as much close as possible (the nodes of contact element and target element is made co-incident for better convergence). Care should be taken that no elements which come under warning or error criteria. The criteria for measurement include 1.Aspect ratio 2.Warpage 3.Maximum and minimum angle 4.Jacobian etc. The mesh pattern of the cyclic faces of the sector is made same, to apply cyclic symmetry boundary conditions.

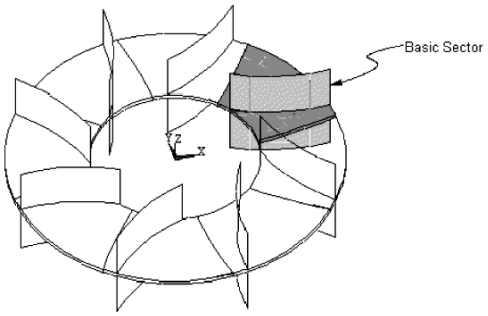

Fig 2.1 Typical rotating disc with basic sector.

2.3 Symmetry boundary conditions

In actual condition both the faces of the cycle, will experience similar stresses and displacements. Hence both the faces should have matching nodes and they are coupled in all degrees of freedom. The couplings achieve symmetry boundary conditions.

Fig 2.2 Boundary condition on basic sector.

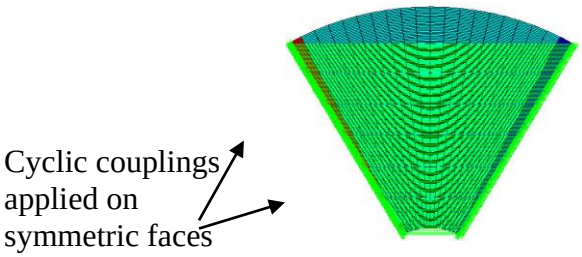

2.4 Constraints

To prevent rigid body motion the rotating disc sector is constrained in axial and hoop directions as shown in the figure 2.3 and figure 2.4.

2.4.1 Axial constraints: The nodes on one face are constrained in axial direction i.e. Uz direction (Fig 2.3).

2.4.2 Hoop Constraints: The nodes on the other faces are constrained in hoop direction i.e. Uy direction as shown in figure 2.4.

(This work is licensed under a Creative Commons Attribution 4.0 International License.)

International Journal of Engineering Research & Technology (IJERT)
ISSN: 2278-0181
Vol. 14, Issue 06, ACSCON - 2026

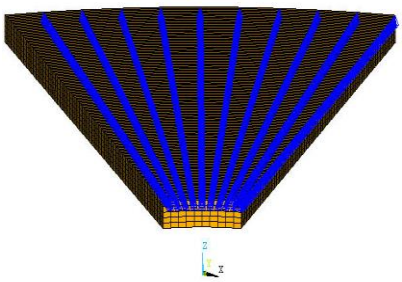

Fig 2.3 Axial constraint

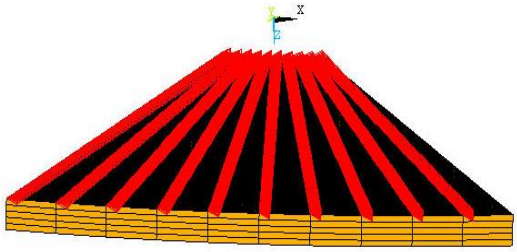

Fig 2.4 Hoop constraint

2.5 Contact simulation

The contact between the shaft and the rotor is simulated by generating contact elements between them and applying required interference as CNOF value, contact surface offset (Real constant number 10 for contact 174).

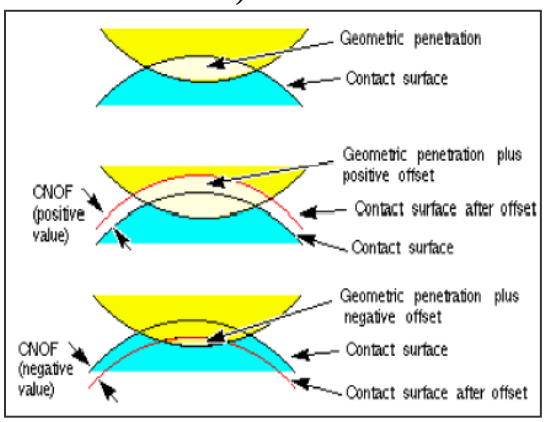

Fig 2.5 Components of True penetration.

3 Equations for stresses and displacements of rotating disc:

3.1 Disc mounted on the shaft with interference

The lames equations for compound cylinder problem can be used to estimate the stresses considering the pressure on the external side as zero i.e. no resistance to expansion from the outside.

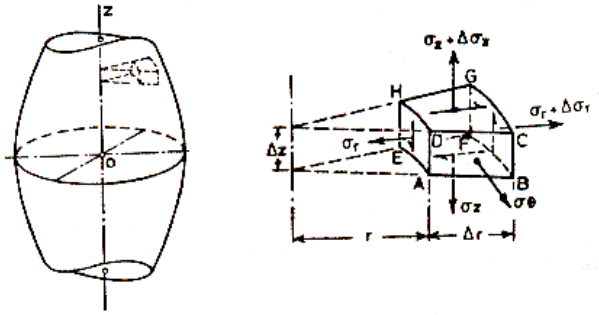

Fig 3.1 cylindrical coordinates of a point and stress on an element

Fig 3.2 cylinder subjected to internal pressure.

3.1.1 Plane stress approach:

We assume that $\sigma_z = 0$, stress in axial direction is zero the equation for radial stress at any location 'r' is given by

$$\sigma_r = \frac{p_a a^2 - p_b b^2}{b^2 - a^2} - \frac{a^2 b^2 (p_a - p_b)}{r^2 (b^2 - a^2)} \quad .....3.1$$

$$\sigma_\theta = \frac{p_a a^2 - p_b b^2}{b^2 - a^2} + \frac{a^2 b^2 (p_a - p_b)}{r^2 (b^2 - a^2)} \quad .....3.2$$

$$\sigma_z = 0 \quad .....3.3$$

Here P_a and P_b are internal and external pressure respectively. The sum of $\sigma_r + \sigma_\theta$ is constant through the thickness of the wall of the cylinder i.e. independent of 'r'. Hence according to Hooks law, the stresses σ_r and σ_θ produce a uniform extension or

(This work is licensed under a Creative Commons Attribution 4.0 International License.)

International Journal of Engineering Research & Technology (IJERT)
ISSN: 2278-0181
Vol. 14, Issue 06, ACSCON - 2026

contraction in Z-direction and cross section perpendicular to the axis of the cylinder remains plane. If we consider two adjacent cross-sections, the deformation undergone by the element does not interfere with the deformation of the neighboring element. Hence, the elements can be considered in the state of plane stress, i.e. $\sigma_z = 0$.

3.1.2 Plane strain condition.

When the cylinder is fairly long sections that are far from the ends can be considered to be in a state of plane strain and we can assume that σ_z does not vary along the Z-axis

$$\sigma_r = \frac{p_a a^2 - p_b b^2}{b^2 - a^2} - \frac{a^2 b^2 (p_a - p_b)}{r^2 (b^2 - a^2)} \quad .....3.4$$

$$\sigma_\theta = \frac{p_a a^2 - p_b b^2}{b^2 - a^2} + \frac{a^2 b^2 (p_a - p_b)}{r^2 (b^2 - a^2)} \quad .....3.5$$

$$\sigma_z = 2\upsilon \frac{p_b a^2 - p_a b^2}{b^2 - a^2} \quad .....3.6$$

The values of σ_r and σ_θ are identical in both plane stress and plane strain condition. But σ_z has a constant value in plane strain condition while it is zero in case of plane stress condition.

3.2 Disc mounted on the rotating shaft without interference:

3.2.1 The equation for radial stress at any location 'r' is given by,

$$\sigma_r = \frac{3+\upsilon}{8} \rho\omega^2 \left[b^2 + a^2 - \frac{a^2 b^2}{r^2} - r^2 \right] \quad ...3.7$$

3.2.2 The equation for circumferential stress at any location 'r' is given by,

$$\sigma_\theta = \frac{3+\upsilon}{8} \rho\omega^2 \left[b^2 + a^2 + \frac{a^2 b^2}{r^2} - \frac{1+3\upsilon}{3+\upsilon} r^2 \right] ....3.8$$

3.2.3 The maximum radial stress is at, $r = \sqrt{ab}$ and is given by,

$$\sigma_{r\max} = \frac{3+\upsilon}{8} \rho\omega^2 (b-a)^2 \quad ...3.9$$

3.2.4 The max circumferential stress is given by,

$$\sigma_{\theta\max} = \frac{3+\upsilon}{4} \rho\varpi^2 \left(b^2 + \frac{1-\upsilon}{3+\upsilon} a^2 \right) \quad ....3.10$$

3.3 Disc mounted on the rotating shaft with interference

The equation for stresses in this case, are not close formed but the stresses will be cumulative of above two cases. The radial stress in case 3.1 are compressive in nature and tend to nullify with tangential stresses from the case 3.2. The Hoop stresses are tensile in both the cases and the stresses will increase as a result of stress accumulation.

3.4 Effect of increase in outer diameter of the disc

As the diameter increases, there is a mass increase as well as radius increases, consequently the radial force on the disc increases as

$$F = mr\omega^2 \quad .....3.11$$

Where F is radial force, m mass of disc, r radius of disc and ω angular velocity of the disc. As a result there will be proportionate increase in the stress.

3.5 Effect of increasing disc speed

As the speed increases, force is squared, consequently the radial force on the disc increases as given in equation 3.11. If a stress s_1 is determined at speed of n_1 rpm and is desired to know the stress s_2 at the speed n_2 rpm the fallowing expression can be manipulated to determine the desired quantity.

$$\frac{s_1}{s_2} = \frac{n_1^2}{n_2^2} \quad .....3.12$$

4. Results and Discussion

The creation of geometry, discretization and application of boundary conditions was done by creating a macro using ANSYS Parametric Design Language

(This work is licensed under a Creative Commons Attribution 4.0 International License.)

International Journal of Engineering Research & Technology (IJERT)
ISSN: 2278-0181
Vol. 14, Issue 06, ACSCON - 2026

(APDL) as it provides greater flexibility of changing geometry and loads.

A portion of disc can be modeled, instead of full disc using cyclic symmetry, which in turn saves computation time as number of elements reduces. The macro can be run for different diameters of disc and different magnitude of loads but for the sake of calculations and result interpretation following geometry and loading conditions are chosen.

Geometry	
Inner diameter of disc	150 mm
Outer diameter of disc	750 mm
Thickness of disc	10 mm
Material properties (Standard Steel)	
Modulus of Elasticity	210000 MPa
Density	7.85e-09 Tonnes/mm^3
Poisson's Ratio	0.29
Loads	
Speed	10000 rpm
Interference	0.2 mm

We will investigate the behavior of the rotating disc for the following cases Using cyclic symmetry boundary condition:

1. Disc mounted on the shaft with interference.
2. Disc mounted on the rotating shaft without interference.
3. Disc mounted on the rotating shaft with interference.
4. Effect of increasing the outer diameter of the disc.

Effect of increasing disc speed

4.1 Disc mounted on the shaft with interference

The maximum contact pressure is 298.6, with entire area in contact with shaft having pressure in the range of 265.422 to 298.6.Thus the FEA result agrees with the theoretical calculation which is given by

$$\frac{E\Delta}{2c}\frac{\left(b^2-c^2\right)}{\left(b^2\right)}=\frac{210000\times 0.2\times[(375)^2-(75)^2]}{2\times(75)\times(375)^2}=268.8\ \text{MPa}$$

C = inner radius of disc (mm), b= outer radius of the disc (mm), △= interference (mm)

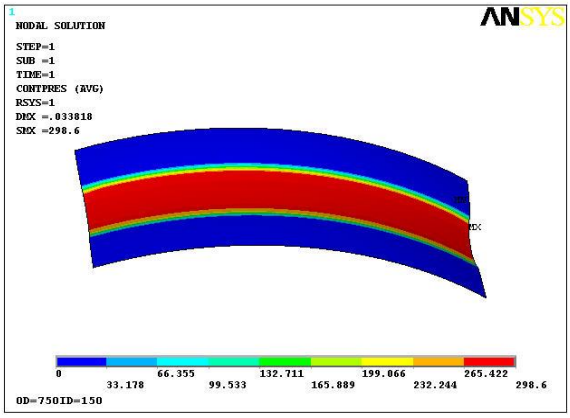

Fig 4.1 Contact Pressure Plot

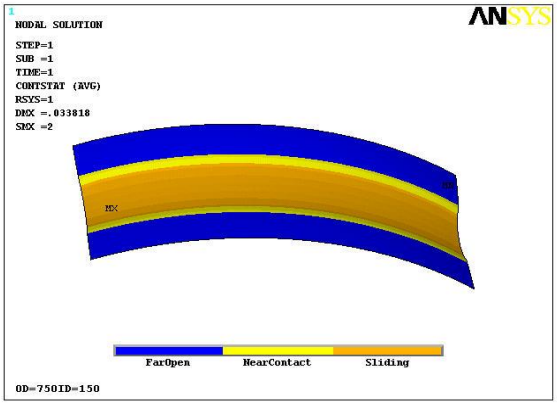

Fig 4.2 Contact status plot.

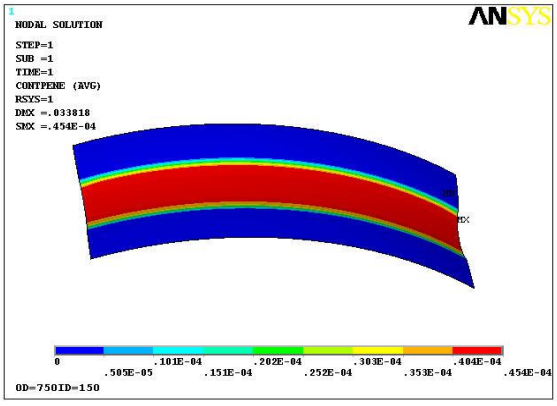

Fig 4.3 Contact penetration plot.

The contact status plot gives information on whether the disc is in contact with the shaft,

(This work is licensed under a Creative Commons Attribution 4.0 International License.)

International Journal of Engineering Research & Technology (IJERT)
ISSN: 2278-0181
Vol. 14, Issue 06, ACSCON - 2026

as contact elements are generated between the interface of the shaft and the disc. The contact penetration plot gives the information about how correct the contact simulation was done by fixing the value of contact stiffness, lower the penetration better is the contact result accuracy. Also the plots for radial stress, circumferential stress, axial stress, equivalence stress and radial displacements were obtained.

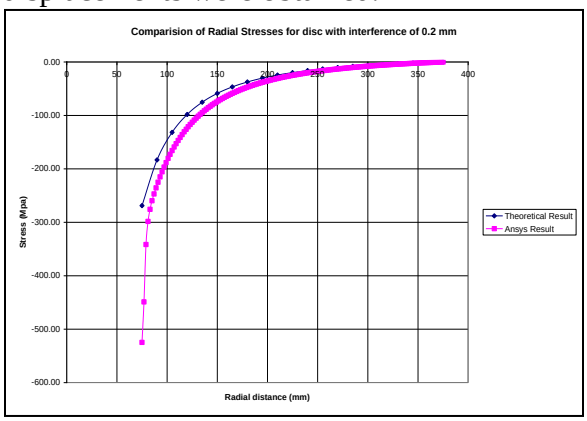

Fig4.4 Comparison of radial stress, analytical and ANSYS result.

The graph shows the stresses using FEA are quite large near the inner radius as result of interference. The graph matches well in region other than inner radius.

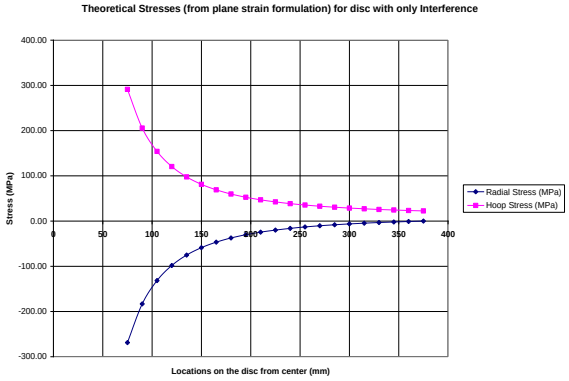

Fig4.5 Theoretical stress distribution.

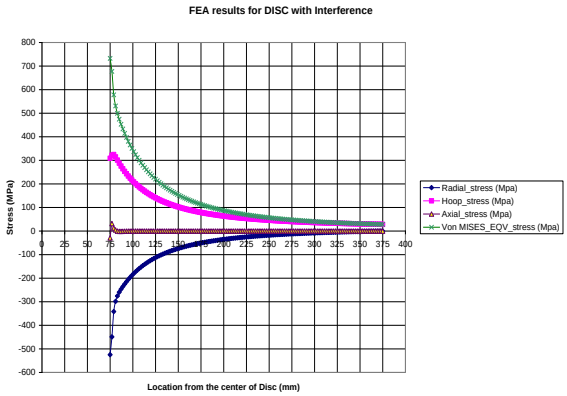

Fig4.5 Stress distribution from FEA results.

4.2 Disc mounted on the rotating shaft without interference.

The max radial stress is given by equation 3.9 gives $\sigma_{r\max}$ = 319.590 MPa.

The max circumferential stress is given by equation 3.10 gives $\sigma_{\theta\max}$ = 1007.1920 MPa.

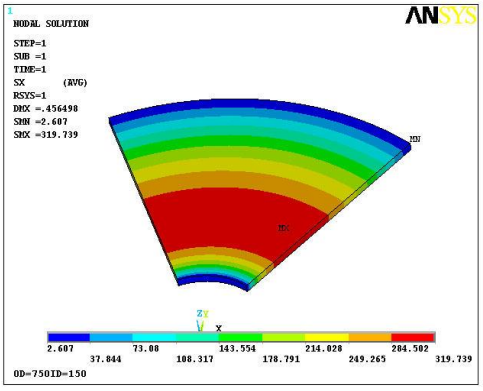

Fig 4.6 Radial stress plot for case 2.

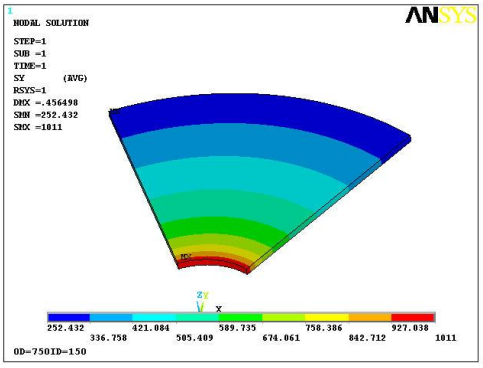

Fig 4.7 Circumferential stress plot for case 2.

(This work is licensed under a Creative Commons Attribution 4.0 International License.)

International Journal of Engineering Research & Technology (IJERT)
ISSN: 2278-0181
Vol. 14, Issue 06, ACSCON - 2026

The Maximum radial stress is 319.739 MPa which matches with theoretical value of 319.59 MPa. The max circumferential stress is 1011 Mpa which matches with Theoretical value of 1007 Mpa

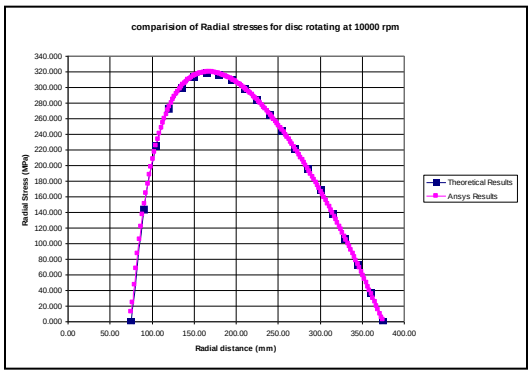

Fig 4.8 Graph of Radial stress against Radial distance

.

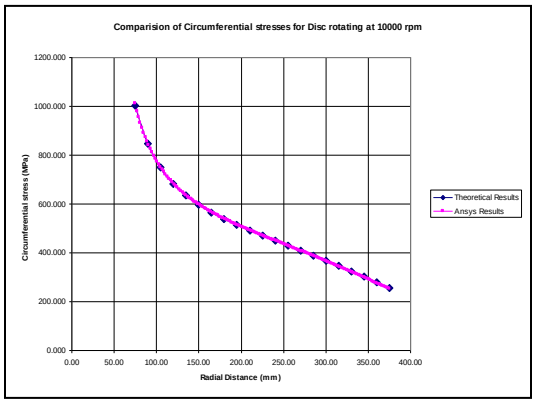

Fig 4.9 Graph of circumferential stress against radial distance

The graph of Radial stress and circumferential stress shows very good convergence of ANSYS result with the Theoretical results.

4.3 Disc mounted on the rotating shaft with interference.

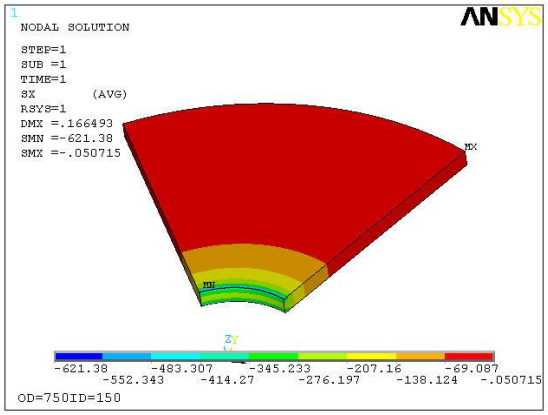

Fig 4.10 Radial stress plot for case 3.

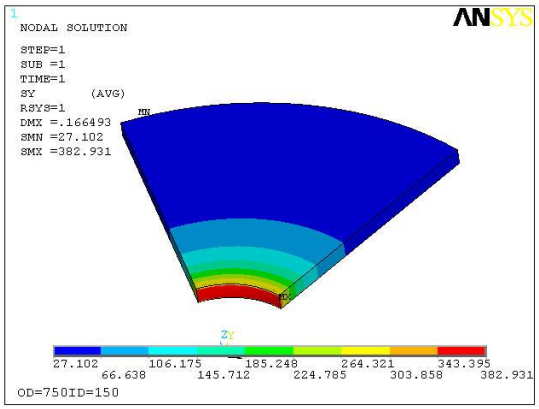

Fig 4.11 Circumferential stress plot for case 3

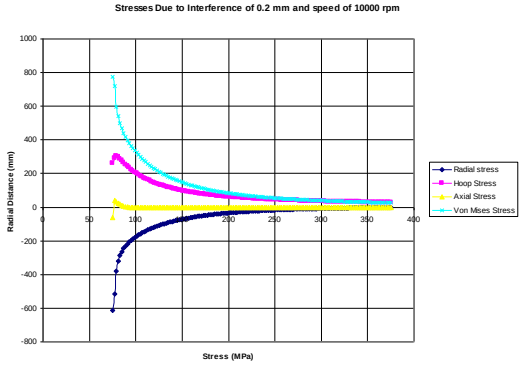

Fig 4.12 Graph showing variation of stress in radial direction for case 3.

The maximum radial stress is 621 MPa and is compressive in nature, the maximum circumferential stress is 382 MPa and is tensile in nature, maximum axial stress 60.21 MPa, maximum Equivalent stress 803 Mpa. The maximum radial displacement 0.16647 mm and total displacement of 0.14449 mm was obtained.

(This work is licensed under a Creative Commons Attribution 4.0 International License.)

International Journal of Engineering Research & Technology (IJERT)
ISSN: 2278-0181
Vol. 14, Issue 06, ACSCON - 2026

4.4 Effect of increasing the outer diameter of the disc.

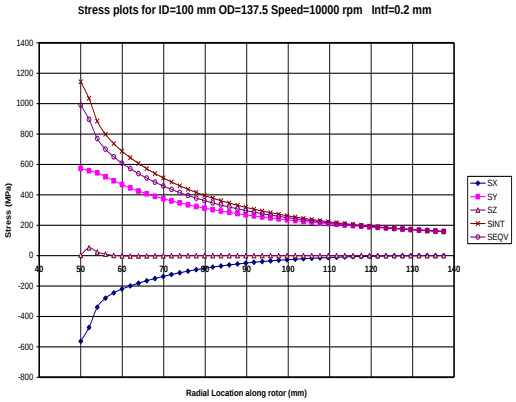

Fig 4.13 Graph showing variation Stresses in radial direction for Outer diameter 137.5 mm.

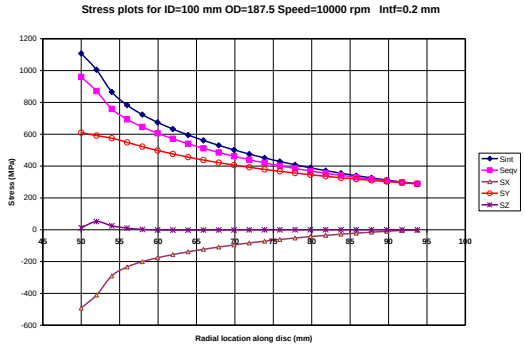

Fig 4.13 Graph showing variation Stresses in radial direction for Outer diameter 187.5 mm.

In this case stress plots were obtained by changing the outer diameter of the disc and it was found that stress increases as the outer diameter increases.

4.5 Effect of increasing disc speed.

As the speed increases the stress on the disc squares, as given by equation 3.12. Various plots for radial stress and von mises equivalent stress were plotted. Also the graph shows that as the speed increases stress also increases.

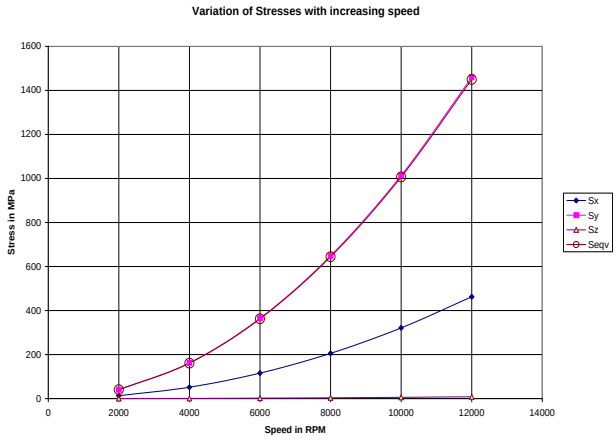

Fig 4.14 Graph showing variation of stress with variation of speed

5. CONCLUSIONS

The rotating disc problem was investigated for stress and displacement. The results of the analysis match closely with the theoretical calculations. For case of rotating disc with interference and speed there are no close formed equations, the FEA results predict the stresses and displacements. This paper focuses on a simple problem and gives elaborate treatment that can form the basis for design of rotating equipment. FEA techniques like cyclic symmetry, contact analysis, use of Solid 3D elements, application of couplings etc have been used

The FEA results show a good comparison with the theoretical results for most of the cases. The results can be used to effectively design a rotor which can withstand the loading conditions of speed and interference.

6. REFERENCES

[1]. Eraslan, Yusuf, “A parametric analysis of rotating variable thickness elastoplastic annular disks subjected to pressurized and radially constrained boundary conditions”, Turkish J. Eng. Env. Sci. 28 (2004), pp 381-395.

[2]. Ahmet, Eraslan, “A Class of Nonisothermal Variable Thickness Rotating Disk Problems Solved by Hypergeometric Functions”, Turkish J. Eng. Env. Sci.29 (2005), pp 241 - 269.

[3]. Fernando viegas stump, Glaucio hermogenes paulino and Emýlio carlos nelli silva, “Material distribution design of functionally graded rotating disks with stress constraint”, 6th world congresses of structural and multidisciplinary optimization, 30 may - 03June 2005, Brazil.

(This work is licensed under a Creative Commons Attribution 4.0 International License.)

International Journal of Engineering Research & Technology (IJERT)
ISSN: 2278-0181
Vol. 14, Issue 06, ACSCON - 2026

[4]. D. W. Cameron,P. R. Geise J. S. Abbott, “Establishing Overspeed Limits for Centrifugal Compressor Impellers”, (Technical paper) Dresser-Rand Inc.
[5]. .L.S.Srinath, “Advanced mechanics of solids”,Tata McGraw Hill, 2003.
[6]. Joseph.E.,Shigley, “Design of Machine Element”,Tata Mc Graw Hill, 2003.
[7]. Desai, Abel, “Introduction to Finite Element Method”, C B S Publishers and distributors, 2004.
[8]. Chandrupatla & Belegundu, “Introduction to Finite Elements in engineering”, Prentice Hall of India Pvt Ltd, 1997.
[9]. V.k.Manicka selvam,Cook “Concepts of Finite Element Method”,John Wiley & Sons,Inc, 2002.
[10]. Egor.P. Popov, “Engineering Mechanics of Solids”, Prentice Hall of India Pvt Ltd, 1986.

(This work is licensed under a Creative Commons Attribution 4.0 International License.)